A Database of Thermodynamic Quantities for the Reactions of Glycolysis and the Tricarboxylic Acid Cycle†

X. Li,‡ R. K. Dash,‡ R. K. Pradhan,‡ F. Qi,‡ M. Thompson,‡ K. C. Vinnakota,‡ F. Wu,‡ F. Yang,§ and D. A. Beard*,‡

Department of Physiology, Medical College of Wisconsin, 8701 Watertown Plank Road, Milwaukee, Wisconsin 53226, and Lilly Singapore Centres for Drug Discovery Pte Ltd, 8A Biomedical Grove, #02-05 Immunos, Singapore 138648

Received: November 30, 2009; Revised Manuscript Received: March 30, 2010

Analysis of biochemical systems requires reliable and self-consistent databases of thermodynamic properties for biochemical reactions. Here a database of thermodynamic properties for the reactions of glycolysis and the tricarboxylic acid cycle is developed from measured equilibrium data. Species-level free energies of formation are estimated on the basis of comparing thermodynamic model predictions for reaction-level equilibrium constants to previously reported data obtained under different experimental conditions. Matching model predictions to the data involves applying state corrections for ionic strength, pH, and metal ion binding for each input experimental biochemical measurement. By archiving all of the raw data, documenting all model assumptions and calculations, and making the computer package and data available, this work provides a framework for extension and refinement by adding to the underlying raw experimental data in the database and/or refining the underlying model assumptions. Thus the resulting database is a refinement of preexisting databases of thermodynamics in terms of reliability, self-consistency, transparency, and extensibility.

Introduction

The principles of biochemical thermodynamics are widely applied in biochemical process design and in theoretical/computational analyses of cellular metabolic networks.[1] Thermodynamic data on biochemical reactions may be used to predict the extent of reaction, to optimize product yields, and to calculate the energy requirements of a given reaction.[2] Recent theoretical studies have combined mass-balance (flux-balance) and thermodynamic constraints to determine feasible ranges of metabolite concentrations[3,4] and have combined metabolic and thermodynamic data to determine feasibility of pathway fluxes in genome-scale networks.[5−8] Furthermore, physically realistic simulation of biochemical system kinetics requires integrating data on thermodynamics and kinetics into a coherent self-consistent set of model equations and associated computer codes.[9,10] These and similar applications require estimated values of basic thermodynamic quantities (such as the standard reference changes in enthalpy, entropy, and free energy) associated with biochemical reactions under given conditions.

To date, the field has relied heavily on the work of R. A. Alberty, who has not only made a number of important theoretical contributions but also developed a database of derived thermodynamic data for biochemical reactions.[11] His work provides the most extensive database of thermodynamic properties available (in terms of number of reactions covered), including the reactions of glycolysis, the tricarboxylic acid cycle (TCA), the purine nucleotide cycle, and a number of other pathways.[11−20] Our laboratory, for example, has made extensive use of the Alberty database, with minor additions, in much of our work in this area.[21−23] Yet optimal progress in the field will require significant extension and refinement because the database does not include all biochemical reactions and associated reactants that are involved in cellular metabolism and other key biochemical processes. Furthermore, enthalpy values, which are essential for accounting for temperature effects, are largely missing from current databases. In addition, it is not clear precisely what raw data were used to obtain the values in the Alberty database. This is a critical issue for several reasons. First, calculation of the formation properties from the raw data requires determination of the solution properties (ionic strength, free metal cation concentrations) associated with the raw experimental data. These determinations often require invoking approximations and making related decisions in a case-specific manner. Second, because the calculated formation properties are interrelated, the database of formation properties may be rigorously extended only by recalculating the entire database using all of the raw data.

Goldberg and colleagues have compiled an extensive database of biochemical thermodynamic data that provide the opportunity to build a large-scale extensible database of biochemical thermodynamic properties.[20,24] Their efforts include carefully evaluating and tabulating thermodynamic data and experimental conditions reported in an enormous number of studies (over 1000 original papers) into a database of thermodynamic measurements on enzyme catalyzed reactions[2,20,25−30] and analyzing subsets of these raw data to estimate the species formation free energies, enthalpies, entropies, and heat capacities.[24] (The raw data are apparent equilibrium constants measured under various biochemical conditions; the derived properties are free energies and enthalpies of formation of chemical species at standard reference conditions.)

The goal of the current work is to present a novel database of thermodynamic properties for the reactions of glycolysis and the tricarboxylic acid cycle (25 total reactions), based on the raw data compiled by Goldberg and colleagues. Thus, like the Alberty database, this initial effort represents only a fraction of

† Part of the "Robert A. Alberty Festschrift".
‡ Medical College of Wisconsin.
§ Lilly-Singapore Centre for Drug Discovery Pte Ltd.

10.1021/jp911381p
Published on Web 05/06/2010

the reactions accounted in the Goldberg data set. Yet our database represents a refinement to the Alberty database in that it accounts for the ionic strength and interactions of biochemical reactants and metal cations (Mg^{2+}, Ca^{2+}, Na^{+}, and K^{+}) in estimating the derived properties from the raw data. Accounting for this level of detail requires estimating the solutions properties (ionic strength, pH, and concentrations of metal cations) associated with each biochemical measurement used in the raw database. Crucially, to make the database extensible, we make the raw data and our documented estimations of solution properties electronically available. Thus, our model represents a framework that may be extended easily and improved in the future by adding more data and/or improving the model assumptions.

Biochemical Thermodynamics Calculations

Derived thermodynamic properties (standard-state Gibbs free energies of formation, $\Delta_f G_i^\circ$, for reference species and reaction enthalpies, $\Delta_r H^\circ$, for reference reactions) may be used to estimate apparent equilibrium constants for biochemical reactions for comparison to experimental data measured under nonstandard conditions. In this work, reference $\Delta_f G_i^\circ$ and $\Delta_r H^\circ$ values are estimated on the basis of minimizing the difference between model predictions and experimental data. This section outlines the basic formulas for converting standard-state reference quantities to account for the experimental state, based on a number of simple thermodynamic models accounting for temperature, ionic screening, and ion binding.[11,31]

Standard-State Properties of Chemical Reference Reaction. The standard state defined as the reference state in this work is temperature $T = 298.15$ K and ionic strength $I = 0$. For each biochemical reactant, a reference species is defined, which is the minimum-cation-bound state considered for a given reactant. (For inorganic phosphate, HPO_4^{2-} is the reference species because our calculations ignore PO_4^{3-}, a species that is present in significant quantities only at pH values above 12) Consider a chemical reference reaction, which is stoichiometrically balanced:[31]

$$0 \rightleftharpoons \sum_{i=1}^{N} \nu_i A_i \tag{1}$$

where N is the total number of species and ν_i is the stoichiometric coefficient associated with the species A_i. (The stoichiometric coefficient is negative for species consumed by the reaction, positive for species generated by the reaction.) The standard reaction Gibbs energy and enthalpy can be calculated as follows:

$$\Delta_r G^\circ = \sum_{i=1}^{N} \nu_i \Delta_f G_i^\circ \tag{2}$$

$$\Delta_r H^\circ = \sum_{i=1}^{N} \nu_i \Delta_f H_i^\circ \tag{3}$$

(Here values of species-level $\Delta_f G_i^\circ$ values and reaction-level $\Delta_r H^\circ$ values are estimated because the available data do not allow for estimation of $\Delta_f H_i^\circ$ for the species involved in the reaction studied.)

Temperature and Ionic Interactions. Over the temperature range $T = 273.15-313.15$ K, the effects of temperature (T) and ionic strength (I) on reference reaction Gibbs free energy and enthalpy can be effectively approximated using formulas derived from the van't Hoff relationship and the extended Debye−Hückel theory,[11,31−34] assuming $\Delta_r H^\circ$ is constant over this temperature range. I.e., $\Delta_r H^\circ$ is a function of I only:

$$\Delta_r G^\circ(T_2,I) = \frac{T_2}{T_1}\Delta_r G^\circ(T_1,I=0) + \left(1 - \frac{T_2}{T_1}\right)\Delta_r H^\circ(I=0) - RT_2\alpha(T_2)\frac{I^{1/2}}{1 + BI^{1/2}}\sum_{i=1}^{N}\nu_i z_i^2 \tag{4}$$

$$\alpha(T) = 1.10708 - (1.54508 \times 10^{-3})T + (5.95584 \times 10^{-6})T^2 \tag{5}$$

$$\Delta_r H^\circ(T,I) = \Delta_r H^\circ(T,I=0) + RT^2\beta(T)\frac{I^{1/2}}{1 + BI^{1/2}}\sum_{i=1}^{N}\nu_i z_i^2 \tag{6}$$

$$\beta(T) = \frac{d\alpha}{dT} = -1.54508 \times 10^{-3} + (11.9117 \times 10^{-6})T \tag{7}$$

where I is the ionic strength in molar (M) units, z_i is the valence of species i, and B is an empirical constant taken to be 1.6 $M^{-1/2}$. Here $\alpha(T)$ is the coefficient in the Debye equation $\ln \gamma = -\alpha z^2 I^{1/2}$, where γ is the activity coefficient of a species with valence z; the coefficients of the polynomial expansions $\alpha(T)$ and $\beta(T)$ are obtained from fitting data.[35]

A pK is the negative base-10 logarithm of a dissociation constant K_d; the influence of T and I on a pK value is approximated:[9]

$$pK(T_2,I_2) = pK(T_1,I_1) + \frac{\alpha(T_1)}{2.303}\cdot\left(\frac{I_1^{1/2}}{1 + BI_1^{1/2}} - \frac{I_2^{1/2}}{1 + BI_2^{1/2}}\right)\cdot\sum \nu_i z_i^2 + \frac{\Delta_d H_{K_d}(I_2)}{2.303\cdot R}\cdot\left(\frac{1}{T_2} - \frac{1}{T_1}\right) \tag{8}$$

where $\Delta_d H_{K_d}$ is the dissociation enthalpy.

Ionic Binding. At given T and I, the equilibrium constant, K, for a reference chemical reaction and the apparent equilibrium constant, K', for the associated biochemical reaction are related:[31]

$$K = \exp\left(\frac{-\Delta_r G^\circ}{RT}\right) = \frac{K'}{\prod_{j=1}^{N} P_j^{\nu_j}}\cdot[H^+]^{\nu_H} \tag{9}$$

where P_j is the binding polynomial associated with reactant j (see below) and ν_H is the stoichiometric coefficient associated with H^+ in the reference reaction.

The apparent equilibrium constant defines the equilibrium mass-action ratio of biochemical reactants defined in terms of sums of species. For example, for the ATP hydrolysis reaction

$$H_2O + ATP^{4-} \rightleftharpoons H^+ + HPO_4^{2-} + ADP^{3-}$$

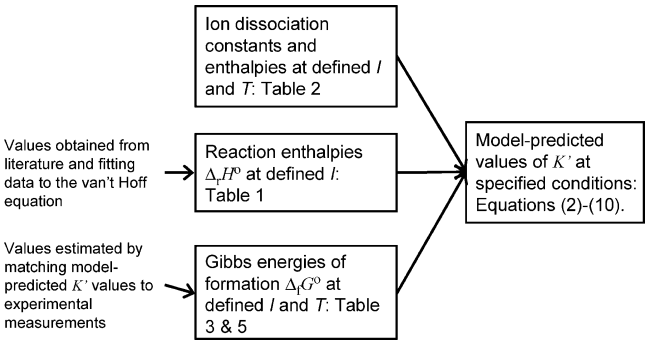

Figure 1. Overview of thermodynamic model calculations.

the apparent equilibrium constant is the mass-action ratio

$$K' = \left(\frac{[\Sigma\mathrm{ADP}][\Sigma\mathrm{Pi}]}{[\Sigma\mathrm{ATP}]}\right)_{\mathrm{eq}}$$

where the notation [Σ•] indicates summation over all species that make up a given reactant. The binding polynomial for a given reactant depends on the free concentrations of hydrogen and metal cations. With pK values corrected for given T and I, the binding polynomial for reactant j is defined:[36]

$$P_j = 1 + \frac{10^{-\mathrm{pH}}}{K_{\mathrm{H1}}} + \frac{10^{-2\mathrm{pH}}}{K_{\mathrm{H1}}K_{\mathrm{H2}}} + \frac{[\mathrm{Mg}^{2+}]}{K_{\mathrm{Mg1}}} + \frac{10^{-\mathrm{pH}}[\mathrm{Mg}^{2+}]}{K_{\mathrm{H1}}K_{\mathrm{HMg}}} + \frac{[\mathrm{Mg}^{2+}]^2}{K_{\mathrm{Mg1}}K_{\mathrm{Mg2}}} + \cdots \quad (10)$$

Each term in the binding polynomial determines the relative amount of reactant j in an associated bound state. For example the fraction of reactant in the single Mg^{2+}-bound state is $[Mg^{2+}]/K_{Mg1}P_j$.

The steps involved in estimating apparent equilibrium constants from species-level thermodynamic properties are illustrated in Figure 1.

Input Data

Database of Measured Equilibrium Constants. Database development starts with compiling measured equilibrium constants for reactions involving reactants from glycolysis and the TCA cycle. The raw experimental data are largely obtained from original reports included in the Goldberg et al. database.[2,25−28] (Data on the ATP hydrolysis reaction are obtained from Rosing et al.,[37] a study that is not listed or evaluated in the Goldberg et al. database. Data on the pyruvate kinase reaction are obtained from Dobson et al.[38] All other sources of data are cited and evaluated in the Goldberg et al. database.) Using this collection of papers, we are able to make use of the critical evaluations of Goldberg et al., which include quality ratings assigned according to the details reported in the individual studies.[2] Specifically, we preferentially selected data evaluated as "A" quality where available for a given reaction. When A-quality data are not available, we have populated the database with B-quality data. (No data rated "C" or "D" are included in the raw-data database.) Since data on some reactions involved in TCA cycle are not available, data on several additional reactions that operate on glycolysis and TCA cycle reactants are included in the calculations. These additional reactions are $NAD(P)^+$ transhydrogenase (EC 1.6.1.1), malic enzyme (EC 1.1.1.40), malate dehydrogenase 2 (EC 1.1.1.37), NAD^+ kinase (EC 2.7.1.23), ATP hydrolysis (EC 3.6.1.32), glucose-6-phosphate hydrolysis (EC 3.1.3.1), and pyruvate carboxylase (EC 6.4.1.1).

Each measurement value compiled in the raw-data database contains the following information: (1) experimental conditions, including temperature, pH, ionic strength, apparent equilibrium constant, free metal cation concentrations, buffer, and experimental method; (2) rating and enzyme (EC number); (3) detailed notes on experiments and strategies of estimations and approximations applied in calculations; (4) reference information. This database includes raw data explicitly reported in the original sources and data derived from the conditions reported in the original sources. Estimates of free cation concentrations and ionic strength typically require invoking assumptions, which are explicitly documented in the database. The raw-data database (Biothermo_Rawdata.xls) is available for download from the Supporting Information; updated versions of the experimental database will be made available at the URL http://www.biocoda.org.

Approximations and calculations associated with two example reaction entries are detailed in Appendix I. These examples show how the ionic species distribution is computed for the experiments on glucose-6-phosphate isomerase (EC 5.3.1.9) and phosphoglycerate mutase (EC 5.4.2.1) reported by Tewari et al.[39] and Guynn[40], respectively.

Database of Reactions and Estimated Standard Reaction Enthalpies. The complete set of reactions studied here is defined in Table 1, with EC numbers, reaction names, and the abbreviations employed, the reference reaction stoichiometries, and estimated standard reaction enthalpies at $T = 298.15$ K, $I = 0$ M. (Recall that a biochemical reactant is made up of a sum of chemical species.[11] The reference species for a given reactant is defined here as the minimal-cation-bound state considered in the calculations.) Here we have adopted the convention that chemical species are expressed with a superscript indicating the charge, even when the charge is zero. This way, for example, the abbreviation for references species for glucose (GLC^0) is distinguished from the abbreviation for the biochemical reactant GLC. The reactant abbreviations are used as variable names in the computer code and therefore do not use subscripts or superscripts.

Reaction enthalpies ($\Delta_r H^\circ$) reported in Table 1 are obtained as follows: When data on apparent equilibrium constants at different temperatures are available, values for reference reaction equilibrium constant are obtained using eq 9. These values are adjusted to $I = 0$ M. Finally, given a set of measures of K at $I = 0$ and different temperatures, $\Delta_r H^\circ(I = 0)/R$ is estimated from the slope of $\ln(K)$ vs $1/T$.[2] Illustrations of this analysis are given in Appendix II. When the raw-data database provides data at only one temperature for a given reaction, values of $\Delta_r H^\circ$ are obtained from Goldberg et al.,[2,25−28] where available. When neither equilibrium data at different temperatures nor prior values of $\Delta_r H^\circ$ are available, the symbol "#" is used to denote the absence of data; for these cases the value is set to be zero in further calculations.

The estimates for $\Delta_r H^\circ$ for certain reactions (FBA, FBA2, and TPI) are based on experimental data obtained at temperatures as high as 333.15 K, which exceeds the valid temperature range of the extended Debye−Hückel theory. Here, the relatively large temperature range facilitates accurate estimates of the slope of $\ln(K)$ vs $1/T$ yet relies on applying the Debye−Hückel theory outside of the reported range of accuracy. Calculations for $\Delta_r H^\circ$ for these reactions are detailed in Appendix II.

TABLE 1: Reactions with Standard Reaction Enthalpies $\Delta_r H°$ Estimated for $I = 0$

EC no.	reaction name	reaction abbrev	reference reaction	$\Delta_r H°$ (kJ/mol)
EC 2.7.1.1	glucokinase	GLK	$GLC^0 + ATP^{4-} = G6P^{2-} + ADP^{3-} + H^+$	−23.8[b]
EC 5.3.1.9	phosphoglucose isomerase	PGI	$G6P^{2-} = F6P^{2-}$	11.53[a]
EC 2.7.1.11	phosphofructokinase	PFK	$F6P^{2-} + ATP^{4-} = F16P^{4-} + ADP^{3-} + H^+$	−9.5[c]
EC 4.1.2.13	fructose-1,6-biphosphatate aldolase	FBA	$F16P^{4-} = DHAP^{2-} + GAP^{2-}$	48.97[a]
EC 5.3.1.1	triosphosphate isomerase	TPI	$GAP^{2-} = DHAP^{2-}$	2.73[e]
EC 4.1.2.13	fructose-1,6-biphosphatate aldolase 2	FBA2	$F16P^{4-} = 2\ DHAP^{2-}$	51.70[a]
EC 1.2.1.12	glyceraldyde-3-P dehydrogenase	GAP	$GAP^{2-} + HPO_4^{2-} + NAD^- = BPG^{4-} + NADH^{2-} + H^+$	#[d]
EC 2.7.2.3	phosphoglycerate kinase	PGK	$GAP^{2-} + HPO_4^{2-} + NAD^- + ADP^{3-} = PG3^{3-} + NADH^{2-} + ATP^{4-} + H^+$	#[d]
EC 5.4.2.1	phosphoglycerate mutase	PGM	$PG2^{3-} = PG3^{3-}$	28.05[a]
EC 4.2.1.11	enolase	ENO	$PG2^{3-} = PEP^{3-} + H_2O^0$	15.1[a]
EC 2.7.1.40	pyruvate kinase	PYK	$PYR^- + ATP^{4-} = PEP^{3-} + ADP^{3-} + H^+$	5.415[b]
EC 4.1.3.7	citrate synthase	CITS	$OAA^{2-} + ACoA^0 + H_2O^0 = CIT^{3-} + COAS^- + 2\ H^+$	#[d]
EC 4.2.1.3	aconitrate hydratese	ACON	$ISCIT^{3-} = CIT^{3-}$	−20.0[a]
EC 1.1.1.42	isocitrate dehydrogenase	IDH	$ISCIT^{3-} + NADP^{3-} + H_2O^0 = AKG^{2-} + NADPH^{4-} + CO_3^{2-} + 2\ H^+$	−22.17[a]
EC 6.2.1.4	succinate-CoA ligase	SCS	$GTP^{4-} + SUC^{2-} + COAS^- + H^+ = GDP^{3-} + HPO_4^{2-} + SUCCoA^-$	−30.9[a]
EC 4.2.1.2	fumarate hydratase	FUM	$FUM^{2-} + H_2O^0 = MAL^{2-}$	−13.18[a]
EC 1.1.1.37	malate dehydrogenase	MDH	$MAL^{2-} + NAD^- = OAA^{2-} + NADH^{2-} + H^+$	51.29[a]
EC 2.7.4.6	nucleoside-diphosphate kinase	NDK	$ATP^{4-} + GDP^{3-} = ADP^{3-} + GTP^{4-}$	#[d]
EC 1.6.1.1	NADP transhydrogenase	NPTH	$NAD^- + NADPH^{4-} = NADH^{2-} + NADP^{3-}$	−4.1[c]
EC 1.1.1.40	malic enzyme	MLE	$MAL^{2-} + NADP^{3-} + H_2O^0 = PYR^- + NADPH^{4-} + CO_3^{2-} + 2\ H^+$	#[d]
EC 1.1.1.37	malate dehydrogenase 2	MDH2	$MAL^{2-} + ACoA^0 + NAD^- + H_2O^0 = CIT^{3-} + COAS^- + NADH^{2-} + 3\ H^+$	#[d]
EC 2.7.1.23	NAD^+ kinase	NADK	$ATP^{4-} + NAD^- = ADP^{3-} + NADP^{3-} + H^+$	#[d]
EC 3.6.1.32	ATPase	ATPS	$ATP^{4-} + H_2O^0 = ADP^{3-} + HPO_4^{2-} + H^+$	−20.5[b]
EC 3.1.3.1	alkaline phosphatase/G6P hydrolysis	G6PH	$G6P^{2-} + H2O^0 = GLC^0 + HPO_4^{2-}$	0.91[b]
EC 6.4.1.1	pyruvate carboxylase	PCL	$PYR^- + ATP^{4-} + CO_3^{2-} = OAA^{2-} + ADP^{3-} + HPO_4^{2-}$	#[d]
EC 1.2.4.1 + EC 2.3.1.12 + EC 1.8.1.4	pyruvate dehydrogenase complex	PDH	$PYR^- + COAS^- + NAD^- + H_2O = CO_3^{2-} + ACoA^0 + NADH^{2-} + H^+$	#[d]
EC 1.1.1.41	isocitrate dehydrogenase	IDH2	$ISCIT^{3-} + NAD^- + H_2O^0 = AKG^{2-} + NADH^{2-} + CO_3^{2-} + 2\ H^+$	−26.27[e]
EC 1.2.1.52	α-ketoglutarate dehydrogenase	AKGDH	$AKG^{2-} + NAD^- + COAS^- + H_2O^0 = SUCCoA^- + NADH^{2-} + CO_3^{2-} + H^+$	#[d]
EC 1.3.5.1	succinate dehydrogenase	SDH	$SUC^{2-} + CoQ^0 = FUM^{2-} + CoQH_2^0$	#[d]

[a] Calculated value based on experimental data at different temperatures. [b] Goldberg et al.[25,26] [c] Values obtained from Goldberg et al.[2,25] where associated ionic strength is not reported. [d] Value not available. [e] Value calculated from the sum of dependent reactions.

Database of Reactant and Dissociation Constants. Table 2 lists the basic thermodynamic and ion binding data for biochemical reactants and associated reference species. The format of Table 2 is similar to the reactant database included in the BISEN package recently distributed by our group.[41] For each reactant entry the following information is provided: (1) detailed name of reactant; (2) reference species abbreviation; (3) reactant abbreviation; (4) charge of reference species; (5) number of protons in reference species; (6) the dissociation constants (provided as pK) and the corresponding dissociation enthalpies $\Delta_d H_{K_d}$. Dissociation constants and enthalpies are tabulated at 298.15 K and 0.1 M ionic strength. The symbol "#" is used to indicate the absence of data. For these cases, the pK's are assumed to be infinite (no binding) with corresponding dissociation constants equal to zero. The dissociation enthalpy $\Delta_d H_{K_d}$ is set to be zero in the cases where data are not available.

In Table 2, subscripts on "pK" and "$\Delta_d H$" entries are defined as follows: "H", hydrogen; "Mg", magnesium; "K", potassium; "Na", sodium; "Ca", calcium; "1", first ion dissociation; "2", second ion dissociation; "HMg", hydrogen ion binds to the ligand before magnesium ion binds to the ligand. Thus the binding polynomial for ATP is computed

$$P_{ATP} = 1 + \frac{10^{-pH}}{K_{H1}} + \frac{10^{-2pH}}{K_{H1}K_{H2}} + \frac{[Mg^{2+}]}{K_{Mg1}} + \frac{10^{-pH}[Mg^{2+}]}{K_{H1}K_{HMg}} + \frac{[Mg^{2+}]^2}{K_{Mg1}K_{Mg2}} + \frac{[K^+]}{K_{K1}} + \cdots$$

pH is defined on the basis of the activity of free hydrogen ion a_{H^+}, rather than its concentration $[H^+]$. Thus, $pH = -\log_{10}(a_{H^+}) = -\log_{10}([H^+]\cdot\gamma_{H^+})$, where γ_{H^+} is the activity coefficient for hydrogen ion. In all calculations herein, it is assumed that hydrogen-ion dissociation constants are measured relative to 10^{-pH}, not relative to free hydrogen ion concentration.

The values of $\Delta_f G_i°$ in Table 5 are estimated on the basis of the analysis described below.

Estimation of Standard-State Thermodynamic Quantities

The thermodynamic model, implemented in MATLAB (Mathworks, Inc.), provides a general and extendable framework allowing for easy access and modification. Reference $\Delta_f G_i°$ values for the reference species are estimated by minimizing the least-squares difference between model predictions and measured K' values (weighted in inverse proportion to the number of data points available for a given reaction). For the network of 25 reactions for which data are available (the first 25 reactions listed in Table 1), model fitting is based on a total of 620 data entries. There are 21 stoichiometrically independent reactions in this set of 25 reactions. In other words, the stoichiometric matrix for the 25-reaction set has a rank of 21; values of $\Delta_f G_i°$ may be estimated from data on these reactions for 21 references species. Since there are in total 33 reactants in our system, we are unable to independently estimate standard free energies of formation for all the reference species. Thus the values of $\Delta_f G_i°$ for 12 species are set to fixed values, as indicated in Table 3. Values for these 12 entries are obtained from Alberty.[11] (Values of $\Delta_f G_i°$ for CoQ^0 and $CoQH_2^0$ do not

TABLE 2: Reactant Database[a]

reactant	reference species abbrev	reactant abbrev	z_i[b]	N_H[b]	pK_{H1}	$\Delta_d H_{H1}$	pK_{H2}	$\Delta_d H_{H2}$
acetyl-coenzyme A	$ACoA^0$	ACoA	0	3	#	#	#	#
adenosine diphosphate	ADP^{3-}	ADP	−3	12	6.496	−2	3.87	16
adenosine triphosphate	ATP^{4-}	ATP	−4	12	6.71	−2	3.99	15
1,3-bisphosphoglycerate	BPG^{4-}	BPG	−4	4	7.1[c]	#	#	#
citrate	CIT^{3-}	CIT	−3	5	5.67	−1.9	4.35	3.1
coenzyme A-SH	$COAS^-$	COAS	−1	0	8.17[c]	#	#	#
carbon dioxide (total)	CO_3^{2-}	CO2_tot	−2	0	9.9[c]	16.1[c]	6.15[c]	8.27[c]
dihydroxyacetone phosphate	$DHAP^{2-}$	DHAP	−2	5	5.9	#	#	#
D-fructose 6-phosphate	$F6P^{2-}$	F6P	−2	11	5.89	−0.559[d]	1.1	#
D-fructose 1,6-phosphate	$F16P^{4-}$	F16P	−4	10	6.64	#	5.92	#
fumarate	FUM^{2-}	FUM	−2	2	4.09	−1.56	2.86	1.08
D-glucose 6-phosphate	$G6P^{2-}$	G6P	−2	11	5.89[g]	−0.559[d]	#	#
D-glyceraldehyde 3-phosphate	GAP^{2-}	GAP	−2	5	5.27[c]	#	#	#
guanosine diphosphate	GDP^{3-}	GDP	−3	12	6.505	−2.14	2.8	#
D-glucose	GLC^0	GLC	0	12	#	#	#	#
guanosine triphosphate	GTP^{4-}	GTP	−4	12	6.63	−3	2.93	7.1
water	H_2O^0	H2O	0	2	#	#	#	#
isocitrate	$ISCIT^{3-}$	ISCIT	−3	5	5.765	#	4.29	#
α-ketoglutarate	AKG^{2-}	AKG	−2	4	#	#	#	#
malate	MAL^{2-}	MAL	−2	4	4.715	−0.58	3.265	3.4
NAD	NAD^-	NAD_ox	−1	26	#	#	#	#
NADH	$NADH^{2-}$	NAD_red	−2	27	#	#	#	#
NADP	$NADP^{3-}$	NADP_ox	−3	25	#	#	#	#
NADPH	$NADPH^{4-}$	NADP_red	−4	26	#	#	#	#
oxaloacetate	OAA^{2-}	OAA	−2	2	3.9	5.24	2.26	16.62
orthophosphate	HPO_4^{2-}	Pi	−2	1	6.78	4.6	1.945	−8.7
2-phospho-D-glycerate	$PG2^{3-}$	PG2	−3	4	7	#	3.55	#
3-phospho-D-glycerate	$PG3^{3-}$	PG3	−3	4	6.89[c]	#	3.64[e]	#
phosphoenolpyruvate	PEP^{3-}	PEP	−3	2	6.245	#	3.45	#
pyruvate	PYR^-	PYR	−1	3	2.26	12.8	#	#
succinate	SUC^{2-}	SUC	−2	4	5.275	0.41	4.02	3
succinyl-CoA	$SUCCoA^-$	SUCCoA	−1	4	3.99[c]	#	#	#
ubiquinone (oxidized)	CoQ^0	CoQ	0	90	#	#	#	#
ubiquinone (reduced)	$CoQH_2^0$	CoQH2	0	92	#	#	#	#

reactant abbrev	pK_{Mg1}	$\Delta_d H_{Mg1}$	pK_{HMg}	$\Delta_d H_{HMg}$	pK_{Mg2}	$\Delta_d H_{Mg2}$	pK_{K1}	$\Delta_d H_{K1}$
ACoA	#	#	#	#	#	#	#	#
ADP	3.3	−15	1.59	−7.5	1.27	−11.76	1	#
ATP	4.28	−18	2.32	−9.6	1.7	−17.52	1.17	−1
BPG	#	#	#	#	#	#	#	#
CIT	3.517	−8	1.8	#	#	#	0.6	−3.54
COAS	#	#	#	#	#	#	#	#
CO2_tot	#	#	#	#	#	#	#	#
DHAP	1.57	#	#	#	#	#	#	#
F6P	1.74[g]	−9.72[d]	#	#	#	#	#	#
F16P	2.7	#	2.12	#	#	#	#	#
FUM	#	#	#	#	#	#	#	#
G6P	1.74[b]	−9.72[d]	#	#	#	#	#	#
GAP	#	#	#	#	#	#	#	#
GDP	3.4	−7.1	#	#	#	#	#	#
GLC	#	#	#	#	#	#	#	#
GTP	4.31	−17	2.31	#	#	#	#	#
H2O	#	#	#	#	#	#	#	#
ISCIT	2.625	#	1.43	#	#	#	#	#
AKG	#	#	#	#	#	#	#	#
MAL	1.71	−6.16	0.9[h]	#	#	#	0.18	−2.86
NAD_ox	#	#	#	#	#	#	#	#
NAD_red	#	#	#	#	#	#	#	#
NADP_ox	#	#	#	#	#	#	#	#
NADP_red	#	#	#	#	#	#	#	#
OAA	1.02	#	#	#	#	#	#	#
Pi	1.823	−9.518	0.669	#	#	#	0.5	#
PG2	2.45	#	#	#	#	#	1.18	#
PG3	2.21[f]	#	#	#	#	#	0.87[f]	#
PEP	2.26	#	#	#	#	#	1.08	#
PYR	1.1	#	#	#	#	#	#	#
SUC	1.355	#	0.62	#	#	#	0.43	−2.76
SUCCoA	#	#	#	#	#	#	#	#
CoQ	#	#	#	#	#	#	#	#
CoQH2	#	#	#	#	#	#	#	#

TABLE 2: Continued

reactant abbrev	pK_{Na1}	$\Delta_d H_{Na1}$	pH_{HNa}	$\Delta_d H_{HNa}$	pK_{Ca1}	$\Delta_d H_{Ca1}$	pK_{HCa}	$\Delta_d H_{HCa}$
ACoA	#	#	#	#	#	#	#	#
ADP	1.12	#	#	#	2.86	−9.6	1.48	−6.2
ATP	1.31	0.8	#	#	3.95	−13	2.16	−7.9
BPG	#	#	#	#	#	#	#	#
CIT	0.75	−1	#	#	3.54	−1.2	2.07	#
COAS	#	#	#	#	#	#	#	#
CO2_tot	#	#	#	#	#	#	#	#
DHAP	#	#	#	#	1.38	#	#	#
F6P	#	#	#	#	#	#	#	#
F16P	#	#	#	#	#	#	#	#
FUM	#	#	#	#	0.6	−6.44	#	#
G6P	#	#	#	#	#	#	#	#
GAP	#	#	#	#	#	#	#	#
GDP	#	#	#	#	#	#	#	#
GLC	#	#	#	#	#	#	#	#
GTP	#	#	#	#	3.7	#	#	#
H2O	#	#	#	#	#	#	#	#
ISCIT	#	#	#	#	2.54	#	#	#
AKG	#	#	#	#	#	#	#	#
MAL	0.28	0.4	#	#	1.95	−1.06	1.06	8
NAD_ox	#	#	#	#	#	#	#	#
NAD_red	#	#	#	#	#	#	#	#
NADP_ox	#	#	#	#	#	#	#	#
NADP_red	#	#	#	#	#	#	#	#
OAA	#	#	#	#	1.6	#	#	#
Pi	0.61	#	0.0856	#	1.745	−9.518	0.9212	−10.759
PG2	#	#	#	#	#	#	#	#
PG3	#	#	#	#	#	#	#	#
PEP	#	#	#	#	#	#	#	#
PYR	#	#	#	#	0.8	#	#	#
SUC	0.4212	−2.759	#	#	1.405	−8.939	0.65	−8
SUCCoA	#	#	#	#	#	#	#	#
CoQ	#	#	#	#	#	#	#	#
CoQH2	#	#	#	#	#	#	#	#

[a] Dissociation pK and $\Delta_d H$ are reported for $T = 298.15$ K and $I = 0.1$ M. Unless indicated, values are the average number obtained from the NIST database.[48] Dissociation enthalpies are reported in units of kJ/mol. [b] Alberty.[11] [c] Alberty.[32,49] [d] Tewari et al.[50] [e] Larsson-Raünikiewicz.[51] [f] Merrill et al.[52] [g] G6P and F6P are assumed to have equivalent H^+ and Mg^{2+}-dissociation properties. [h] From NIST database[48] at $T = 293.15$ K.

TABLE 3: Values of $\Delta_f G_i^\circ$ ($T = 298.15$ K, $I = 0$) Used in This Study and Taken from Alberty[11] (Table 3.2)

species	$\Delta_f G_i^\circ$ (kJ/mol)
$ACoA^0$	−188.52
ADP^{3-}	−1906.13
$COAS^-$	0[a]
CO_3^{2-}	−527.81
$G6P^{2-}$	−1763.94
GTP^{4-}	−2768.1
H_2O	−237.19
NAD^-	0[a]
$NADPH^{4-}$	−809.19
HPO_4^{2-}	−1096.1
$SUCCoA^-$	−509.59
H^+	0
CoQ^0	0[a]
$CoQH_2^0$	−89.92

[a] Property value is based on the arbitrary assignment of zero.

come into these calculations.) A weighted simultaneous solution of standard reaction Gibbs energies is obtained for the entire data set by minimizing the difference between model predictions and experimental data. The whole data set is analyzed by a nonlinear least-squares procedure with the *lsqnonlin* solver (Mathworks, Inc.).

Results

Experimental Data Database. The raw-data database is provided in spreadsheet archived as Supporting Information with this paper and is available for download from http://www.biocoda.org. This database contains raw reported apparent equilibrium constants, along with reported data on experimental conditions and estimates of free ion concentrations obtained from reported experimental conditions. All assumptions invoked in assembling this database are detailed in the spreadsheet database.

Estimated Gibbs Free Energies of Formation. Computed values of K' versus experimental measures for all 620 data points are plotted in Figure 2. (Here computed K' values are obtained on the basis of accounting for the biochemical state associated with a given experimental measurement in the raw-data database.) These data span almost 14 orders of magnitude and reveal good agreement between model predictions and measured data. The optimal of estimates $\Delta_r G^\circ$ and $\Delta_f G_i^\circ$ that are associated with these predictions are listed in Tables 4 and 5, compared to the values from Alberty.[11] Some (3 out of 25) of the current model predictions are indistinguishable from predictions based on the $\Delta_f G_i^\circ$ values reported by Alberty, with an absolute difference of less than 0.1 kJ/mol between estimated $\Delta_r G^\circ$ values. Yet there exist significant differences for several entries, with many differences greater than RT at standard temperature.

To compare the predictions based on this database to those based on the Alberty database, computed K' versus experimental measures are plotted in Figures 3−5 for 14 individual reactions. Figure 3 illustrates model predictions versus experimental data for the three reactions (PGI, ENO, and NDK) for which the current database and the Alberty database yield most similar

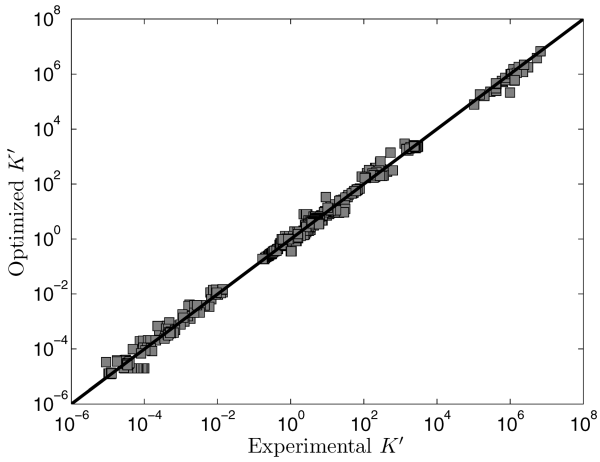

Figure 2. Model-predicted K' vs experimental K'. Model predicted apparent equilibrium constants under defined experimental conditions (T, I, $[Mg^{2+}]$, $[Ca^{2+}]$, $[Na^+]$, $[K^+]$, and pH) are plotted versus experimental measurements for all data in the raw-data database.

results. Thus for these reactions, predictions based on either set of $\Delta_f G_i^\circ$ values (or equivalently $\Delta_r G^\circ$ values) are largely indistinguishable. Note that for these three reactions $\Sigma \nu_i z_i^2 = 0$; thus the ionic interaction terms in eqs 4−8 are zero. In addition, the binding polynomials for the left-hand and right-hand sides of these reactions tend to cancel. For example, for the ENO reaction, the ion dissociation constants for $PG2^{3-}$ and PEP^{3-} have similar values. Thus the computed apparent equilibrium constants for these reactions do not depend strongly on the experimental ionic composition.

TABLE 5: Optimal Predicted $\Delta_f G_i^\circ$ for Reference Species (T = 298.15 K, I = 0 M)

no.	species	$\Delta_f G_i^\circ$ (kJ/mol) (this study)	$\Delta_f G_i^\circ$ (kJ/mol) (from Alberty[11])	absolute difference
1	GLC^0	−916.39	−915.90	0.49
2	ATP^{4-}	−2769.71	−2768.10	1.61
3	$F6P^{2-}$	−1760.81	−1760.80	0.01
4	$F16P^{4-}$	−2597.60	−2601.40	3.80
5	$DHAP^{2-}$	−1292.91	−1296.26	3.35
6	GAP^{2-}	−1285.90	−1288.60	2.70
7	BPG^{4-}	−2354.55	−2356.14	1.59
8	$NADH^{2-}$	23.91	22.65	1.26
9	$PG3^{3-}$	−1507.96	−1502.54	5.42
10	$PG2^{3-}$	−1502.06	−1496.38	5.68
11	PEP^{3-}	−1269.40	−1263.65	5.75
12	PYR^-	−472.72	−472.27	0.45
13	OAA^{2-}	−792.13	−793.29	1.16
14	CIT^{3-}	−1157.52	−1162.69	5.17
15	$ISCIT^{3-}$	−1151.76	−1156.04	4.28
16	$NADP^{3-}$	−836.68	−835.18	1.50
17	AKG^{2-}	−791.57	−793.41	1.84
18	SUC^{2-}	−685.56	−690.44	4.88
19	GDP^{3-}	−1904.53	−1906.13	1.60
20	FUM^{2-}	−598.74	−601.87	3.13
21	MAL^{2-}	−839.30	−842.66	3.36

Figure 4 shows model predictions versus experimental data for the six reactions showing a discrepancy between the current predicted $\Delta_r G^\circ$ values and those obtained on the basis of the

TABLE 4: Optimal Reaction Free Energies for Reference Chemical Reactions ($\Delta_r G^\circ$) and for Biochemical Reactions ($\Delta_r G'^\circ$) under Physiological Conditions[42,43] (T = 310.15 K, I = 0.18 M, pH = 7, $[Mg^{2+}]$ = 0.8 mM, $[K^+]$ = 140 mM, $[Na^+]$ = 10 mM, $[Ca^{2+}]$ = 0.0001 mM)[a]

EC no.	reaction	$\Delta_r G^\circ$ (kJ/mol) (this study)	$\Delta_r G^\circ$(kJ/mol) (from Alberty[11])	absolute difference	$\Delta_r G'^\circ$ (kJ/mol) (physiological conditions)
EC 2.7.1.1	GLK	16.03	13.93	2.10	−19.39
EC 5.3.1.9	PGI	3.13	3.14	0.01	2.79
EC 2.7.1.11	PFK	26.79	21.37	5.42	−15.61
EC 4.1.2.13	FBA	18.80	16.54	2.26	24.64
EC 5.3.1.1	TPI	−7.01	−7.66	0.65	−7.57
EC 4.1.2.13	FBA2	11.79	8.88	2.91	17.07
EC 1.2.1.12	GAP	51.37	51.21	0.16	2.60
EC 2.7.2.3	PGK	34.37	42.84	8.47	−18.99
EC 5.4.2.1	PGYM	−5.90	−6.16	0.26	−6.36
EC 4.2.1.11	ENO	−4.53	−4.46	0.07	−4.46
EC 2.7.1.40	PYK	66.90	70.59	3.69	27.17
EC 4.1.3.7	CITS	60.32	56.31	4.01	−36.43
EC 4.2.1.3	ACON	−5.76	−6.65	0.89	−7.59
EC 1.1.1.42	IDH	97.06	98.00	0.94	−3.32
EC 6.2.1.4	SCS	−56.56	−53.28	3.28	0.05
EC 4.2.1.2	FUM	−3.38	−3.60	0.22	−3.51
EC 1.1.1.37	MDH	71.09	72.02	0.93	27.70
EC 2.7.4.6	NDK	0.01	0	0.01	−0.57
EC 1.6.1.1	NPTH	−3.58	−3.34	0.24	−0.43
EC 1.1.1.40	MLE	103.45	105.76	2.31	0.86
EC 1.1.1.37	MDH2	131.41	128.33	3.08	−6.67
EC 2.7.1.23	NADK	26.90	26.79	0.11	−11.93
EC 3.6.1.32	ATPS	4.67	3.06	1.61	−32.76
EC 3.1.3.1	G6PH	−11.36	−10.87	0.49	−13.27
EC 6.4.1.1	PCL	−24.12	−27.34	3.22	−4.07
EC 1.2.4.1 + EC 2.3.1.12 + EC 1.8.1.4	PDH	17.50	15.78	1.72	−37.49
EC 1.1.1.41	IDH2	93.48	94.66	1.18	−4.81
EC 1.2.1.52	AKGDH	15.28	15.85	0.57	−38.26
EC 1.3.5.1	SDH	−3.10	−1.35	1.75	−2.41

[a] The final four entries (PDH, IDH2, AKGDH, and SDH) represent model predictions for which there are no equilibrium data in the raw data database. Since the $\Delta_f G_i^\circ$ values for CoQ and $CoQH_2$ are not predicted here, these values are set to 0[b] and −89.92 kJ/mol, respectively (from Alberty[11]), to computed $\Delta_r G^\circ$ for the SDH reaction. [b] Property value is based on the arbitrary assignment of zero.

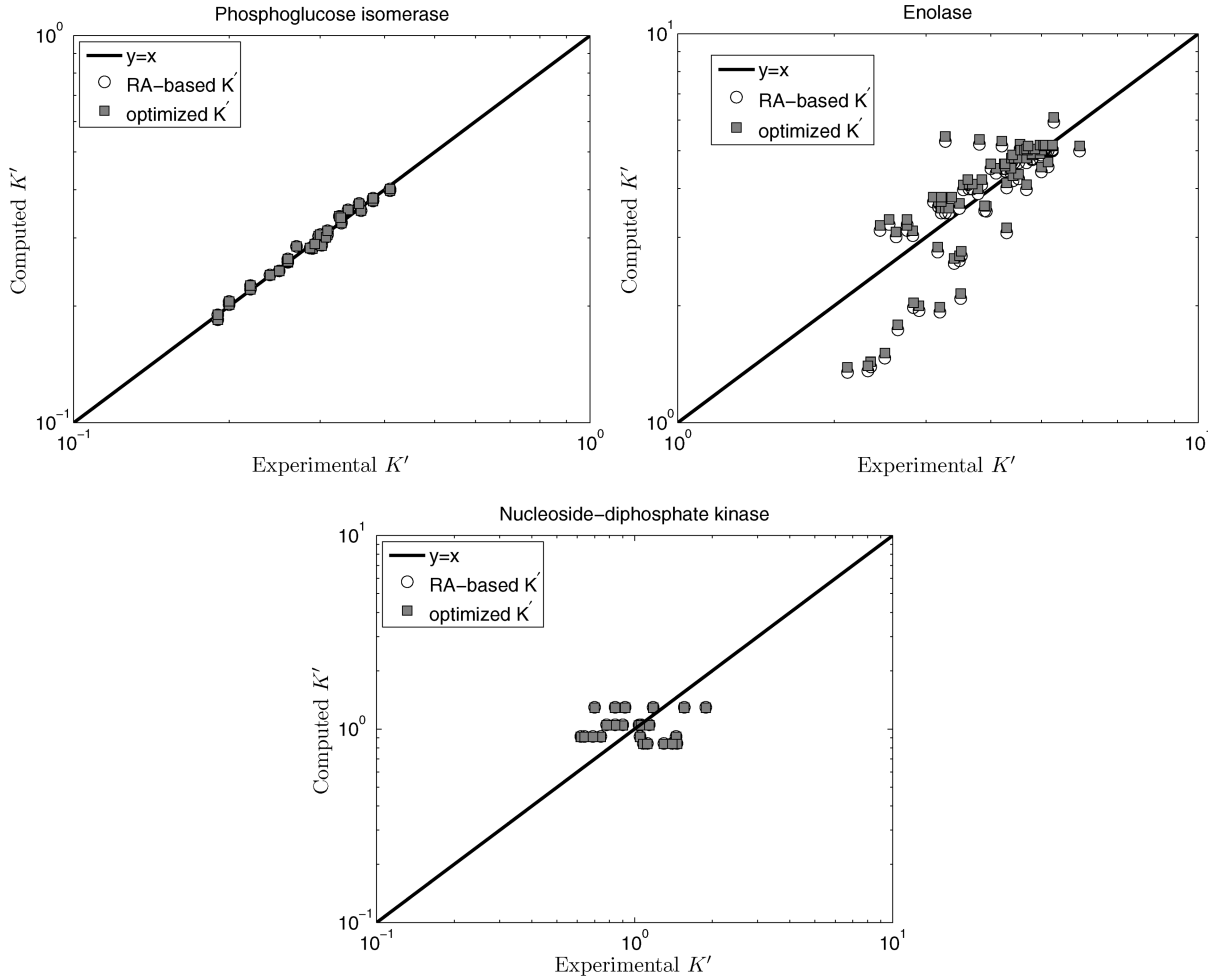

Figure 3. Computed K' vs experimental K' for the phosphoglucose isomerase, enolase, and nucleoside-diphosphate kinase reactions. Open circles (RA-based K') are computed on the basis of the Alberty database;[11] filled squares (optimized K') are computed on the basis of the optimized values of $\Delta_f G_i^\circ$ from Table 5 and the fixed values from Table 3.

Alberty database. For these cases the current model predictions are consistently closer to the experimental data than those obtained from the Alberty free energy values because the predicted K' values depend strongly on the experimental ionic composition. Figure 5 illustrates model predictions for five reactions (PFK, MDH2, NPTH, NADK, and TPI) for which four or fewer data entries are available. For the TPI reaction, model predictions based on the Alberty database are slightly better than those based on the current database.

Predicted Equilibrium Properties. The developed thermodynamic model may be used to estimate equilibrium properties for pyruvate dehydrogenase (PDH), NAD-dependent isocitrate dehydrogenase (IDH2), α-ketoglutarate dehydrogenase (AKGDH), and succinate dehydrogenase (SDH)—reactions in the TCA cycle for which direct measurements are not available in the literature. Since the developed thermodynamic database includes estimates of $\Delta_f G_i^\circ$ for all of the species in these reactions (with the $\Delta_f G_i^\circ$ values in Table 3.2 from Alberty[11]), it is possible to estimate $\Delta_r G^\circ$ and apparent equilibrium properties as functions of ionic strength, temperature, and solution composition.

Table 4 lists the predicted $\Delta_r G^\circ$ values for all reactions. The differences between the current database predictions and those of Alberty for these four reactions (PDH, IDH2, AKGDH, and SDH) are less than RT at standard temperature. Figure 6 plots predicted values of K' as functions of ionic strength for these reactions, assuming $T = 298.15$ K, pH = 7, and no metal cations present. Since the sum of squared charges of products and reactants ($\Sigma \nu_i z_i^2$) is equal to zero in the reaction of SDH, the corresponding K is independent of ionic strength. For this reaction the weak dependence of K' on I is due to the influence of I on the hydrogen ion dissociation constants for succinate and fumarate. For all other reactions, the predicted K' monotonically increases as ionic strength increases because $\Sigma \nu_i z_i^2$ is positive and the increasing ionic strength leads to decreased $\Delta_r G^\circ$ according to eq 4.

Predicted Apparent Gibbs Free Energies under Physiological Conditions. The final column in Table 4 reports the predicted apparent $\Delta_r G'^\circ$ ($= -RT \ln K'$) at physiological conditions representative of a typical mammalian cell[42,43] ($T = 310.15$ K, $I = 0.18$ M, pH = 7, $[Mg^{2+}] = 0.8$ mM, $[K^+] = 140$ mM, $[Na^+] = 10$ mM, $[Ca^{2+}] = 0.0001$ mM). For example, the predicted apparent reference Gibbs free energy ($\Delta_r G'^\circ$) for ATP hydrolysis is −32.76 kJ/mol, which lies between −34.43 kJ/mol (the value obtained from the Alberty database) and the widely used value of −30.5 kJ/mol.[44]

Discussion

We have developed a biochemical thermodynamic database for the reactions of glycolysis and the tricarboxylic acid cycle that is optimally self-consistent and consistent with the data available for these reactions. Theoretical predictions of apparent

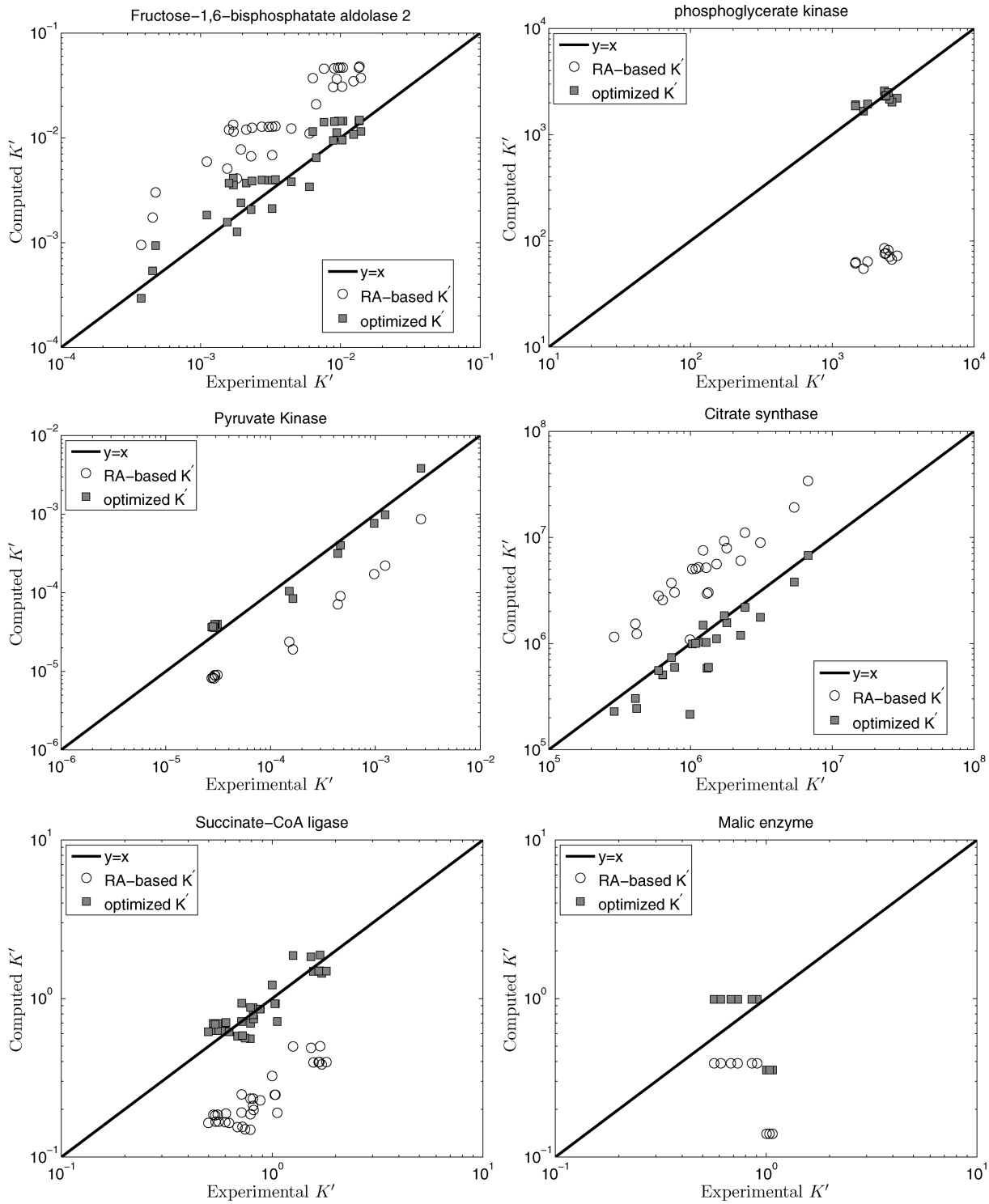

Figure 4. Computed K' vs experimental K' for the fructose-1,6-biphosphatate aldolase 2, phosphoglycerate kinase, pyruvate kinase, citrate synthase, succinate-CoA ligase, and malic enzyme reactions. Open circles (RA-based K') are computed on the basis of the Alberty database;[11] filled squares (optimized K') are computed on the basis of the optimized values of $\Delta_f G_i^\circ$ from Table 5 and the fixed values from Table 3.

equilibrium constants, based on the estimated species-level Gibbs free energies of formation and accounting for the effects of temperature, ionic interactions, and hydrogen and metal cation binding, optimally match experimental data on equilibrium constants.

While this database represents only a small subset of critical biochemical reactions (and indeed a subset of previously available databases, such as that of Alberty[11]), it does improve upon previous works in several ways. First, the underlying model accounts for first- and second-order binding of Mg^{2+}, K^+, Na^+, and Ca^{2+} ions in the experimental media employed in the various studies from which the raw data were obtained. Since the binding of these ions to biochemical reactants has profound effects on apparent equilibria, incorporation of these effects significantly improves the accuracy of the derived database. Second, all raw data and procedures used to estimate quantities such as ionic strength and metal ion concentrations are archived and made

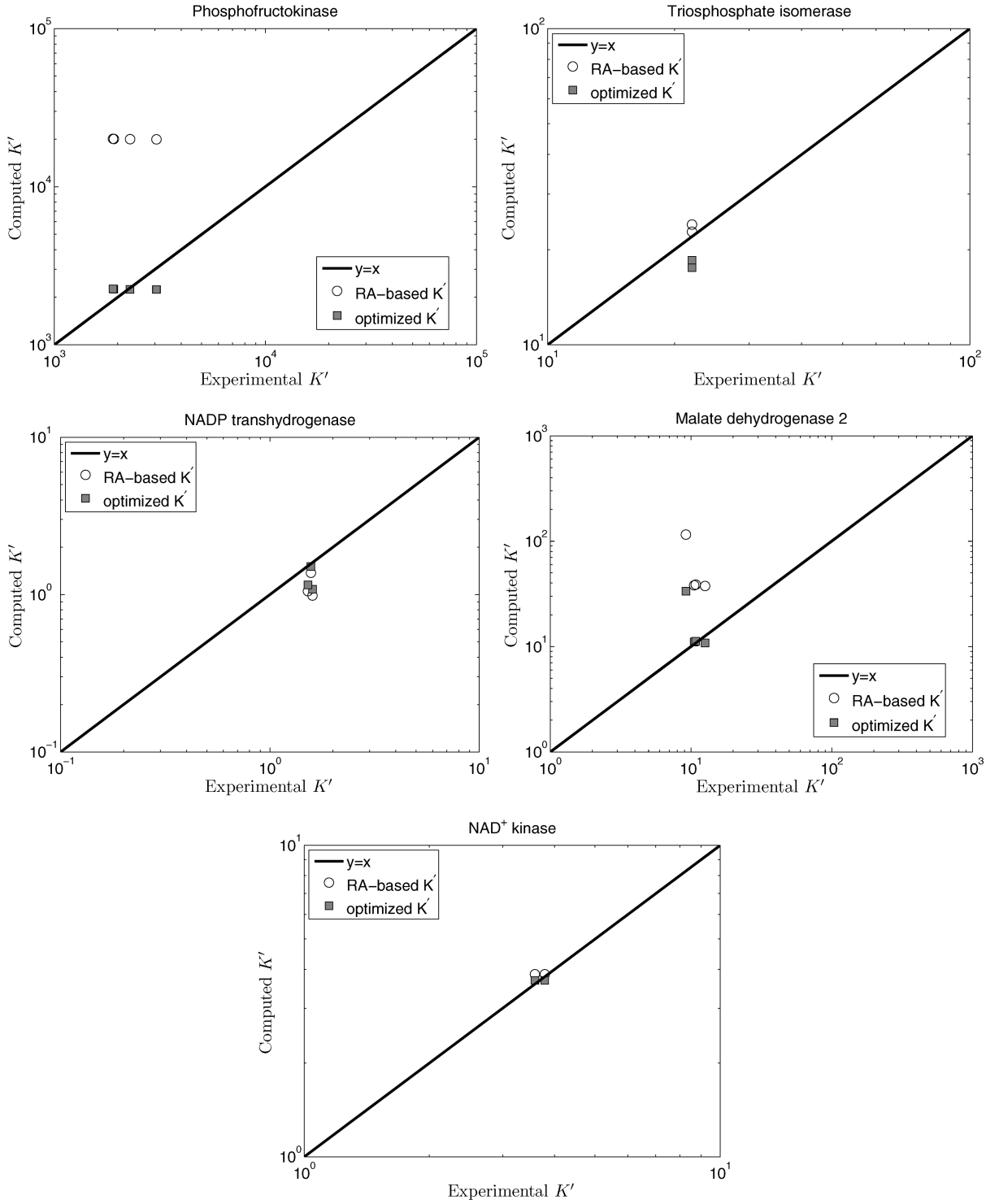

Figure 5. Computed K' vs experimental K' for the phosphofructokinase, triosphosphate isomerase, NADP transhydrogenase, malate dehydrogenase 2, and NAD kinase reactions. Open circles (RA-based K') are computed on the basis of the Alberty database;[11] filled squares (optimized K') are computed on the basis of the optimized values of $\Delta_f G_i^\circ$ from Table 5 and the fixed values from Table 3.

electronically available. The availability of these raw data and computational procedures is crucial to future extensions to the database, since the optimal values of species-level properties are interdependent. Extension of the database to account for reactions (and reactants) not currently in the database will require the recalculation of the entire set of species-level properties.

Third, since the establishment of this database requires invoking certain arbitrary choices, the publication of all underlying data allows those choices to be revised by other investigators. For example, for the ATP hydrolysis reaction, the data of Rosing et al.[37] are used rather than the more extensive data set provided by Phillips et al.[45] Thus, while the model predictions agree well with the data of Rosing et al., they do not match the data of Phillips et al. data as well. We chose to use the data of Rosing et al. in our calculations because these data are more consistent with previously established equilibrium properties for this reaction[11] and because, as Rosing et al. point out, the values of the ATP hydrolysis apparent equilibrium constant of Phillips et al. were based on an inaccurate estimate of the equilibrium

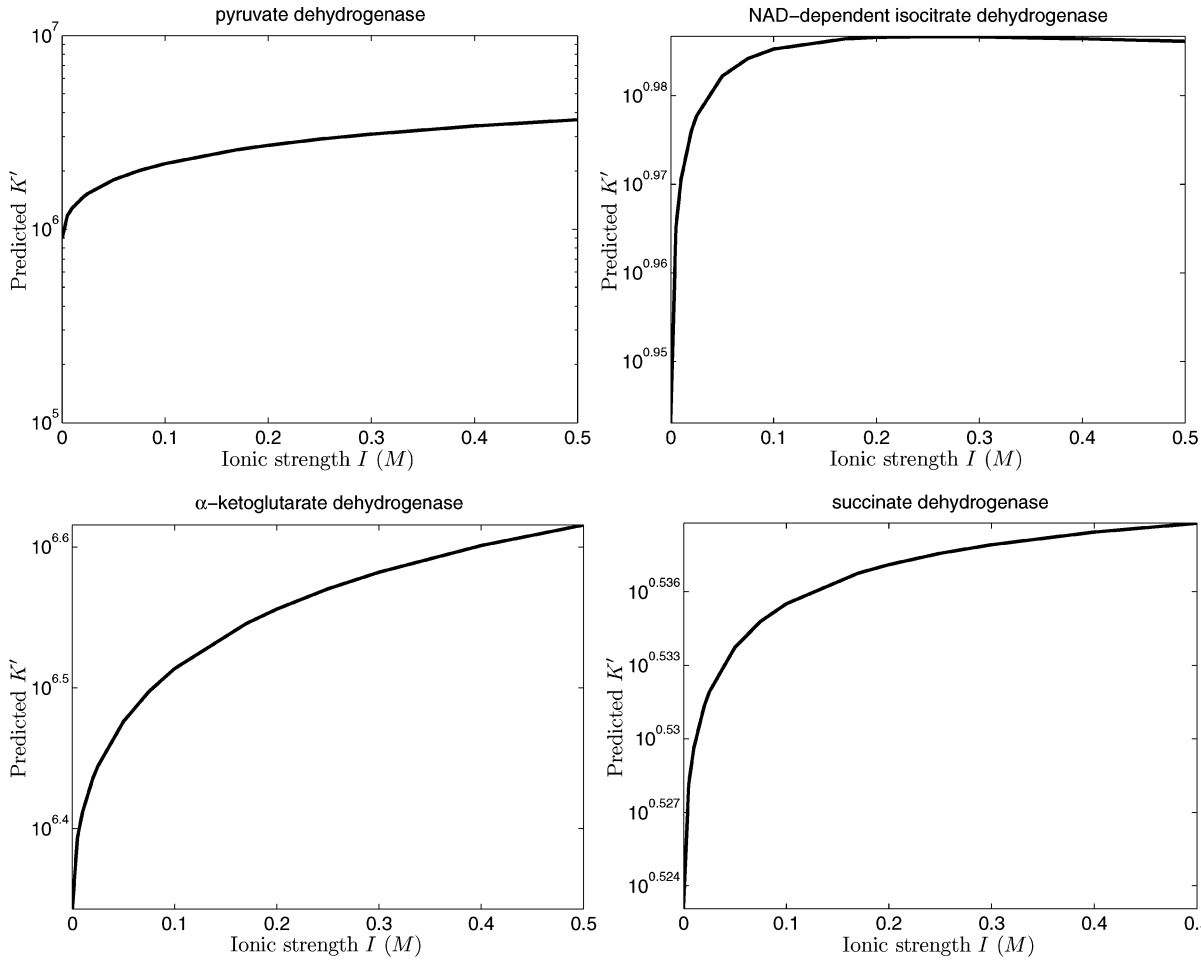

Figure 6. Computed apparent equilibrium constant K' (at 298.15 K) as a function of ionic strength I of the solution pyruvate dehydrogenase, NAD-dependent isocitrate dehydrogenase, α-ketoglutarate dehydrogenase, and succinate dehydrogenase. Calculations assume pH = 7 and no metal cations present.

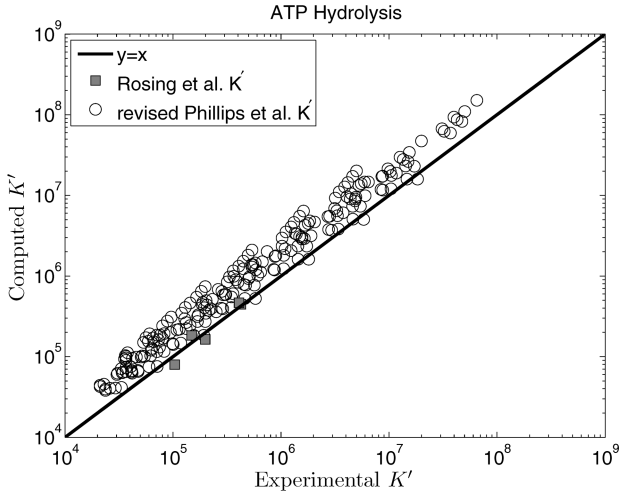

Figure 7. Computed K' vs experimental K' for the ATP hydrolysis reaction. The values reported by Rosing et al.[37] in the original publication are plotted here along with the data of Phillips et al.[45] corrected and rerepublished by Rosing et al.[37]

constant for glutamine synthetase, which was used in a coupled assay for the ATP hydrolysis equilibrium constant. Indeed, Rosing et al. applied a series of corrections to the measurements reported by Phillips et al., yielding the data set plotted in Figure 7, which are much more consistent with the Rosing et al. data and the current model predictions than the original Phillips et al. data set. Using the freely available model code and database developed here, one may easily recalculate a set of species-level properties that are consistent with the corrected Phillips et al. data rather than (or in addition to) the Rosing et al. data.

Therefore this thermodynamic database for glycolysis and the tricarboxylic acid cycle provides a framework for future extensions. To date, efforts in this field have largely relied on the work of the Alberty laboratory. Yet, given the tremendous amount of work that is required in parsing the data published in a given study into a useable form, large-scale extensions will necessarily be a community effort. Goldberg and colleagues have provided a rich and expertly curated database of experimental measurements to build this effort around. Making use of their raw-data database for extending the current database of species-level thermodynamic properties will involve characterizing the ionic composition associated with each data entry that may be used in the network optimization-based estimation of species properties. To do this, each original publication must be studied on a case-by-case basis, case-specific assumptions and approximations determined and documented, and case-specific calculations performed and documented.

Acknowledgment. We are grateful to Robert Goldberg for advice and critical comments. This work was supported by NIH grant HL072011.

Supporting Information Available: Excel file of raw-data database. This material is available free of charge via the Internet at http://pubs.acs.org.

TABLE A1: Experimental Conditions from Tewari et al.[39]

reported conditions					computed total concentrations				
T (K)	pH	[Tris] (M)	[$MgCl_2$] (M)	K'	[Tris·H^+] (M)	$[Cl^-]_{tot}$ (M)	$[Mg^{2+}]_{tot}$ (M)	$[H6P]_{tot}$ (M)	$[Na^+]_{tot}$ (M)
298.15	8.7	0.1	0.001	0.293	0.0191	0.0211	0.0010	0.0445	0.089
298.15	8.7	0.3	0.001	0.299	0.0572	0.0592	0.0010	0.0445	0.089
298.15	8.7	0.64	0.001	0.302	0.122	0.124	0.0010	0.0445	0.089
298.15	8.7	0.1	0.0001	0.287	0.0191	0.0193	0.0001	0.0445	0.089
298.15	8.7	0.1	0.0010	0.293	0.0191	0.0211	0.0010	0.0445	0.089
298.15	8.7	0.1	0.0025	0.308	0.0191	0.0241	0.0025	0.0445	0.089
304.95	8.7	0.1	0.0001	0.310	0.0191	0.0193	0.0001	0.0445	0.089
310.15	8.7	0.1	0.0001	0.329	0.0191	0.0193	0.0001	0.0445	0.089
316.15	8.7	0.1	0.0001	0.357	0.0191	0.0193	0.0001	0.0445	0.089

TABLE A2: Estimated Free Ion Concentrations and Ionic Strength for Data from Tewari et al.[39]

T (K)	pH	[Tris] (M)	[$MgCl_2$] (M)	K'	[$H6P^{2-}$] (M)	[H.H6P$^-$] (M)	[Cl^-] (M)	[Mg^{2+}] (M)	[Na^+] (M)	I (M)
298.15	8.7	0.1	0.001	0.293	0.0438	5.87×10^{-5}	0.0211	3.57×10^{-4}	0.089	0.153
298.15	8.7	0.3	0.001	0.299	0.0438	5.87×10^{-5}	0.0592	3.57×10^{-4}	0.089	0.191
298.15	8.7	0.64	0.001	0.302	0.0438	5.87×10^{-5}	0.124	3.57×10^{-4}	0.089	0.256
298.15	8.7	0.1	0.0001	0.287	0.0444	5.95×10^{-5}	0.0193	3.54×10^{-4}	0.089	0.153
298.15	8.7	0.1	0.0010	0.293	0.0438	5.87×10^{-5}	0.0211	3.57×10^{-4}	0.089	0.153
298.15	8.7	0.1	0.0025	0.308	0.0428	5.75×10^{-5}	0.0241	9.04×10^{-4}	0.089	0.154
304.95	8.7	0.1	0.0001	0.310	0.0444	5.95×10^{-5}	0.0193	3.54×10^{-4}	0.089	0.153
310.15	8.7	0.1	0.0001	0.329	0.0444	5.95×10^{-5}	0.0193	3.54×10^{-4}	0.089	0.153
316.15	8.7	0.1	0.0001	0.357	0.0444	5.95×10^{-5}	0.0193	3.54×10^{-4}	0.089	0.153

TABLE A3: Estimated Free Ion Concentrations and Ionic Strength for Data from Guynn[40]

pH	[$PG3_{tot}$] (mM)	[$PG2_{tot}$] (mM)	[Mg_{tot}] (mM)	[Mg^{2+}] (mM)	[K^+] (mM)	[Cl^-] (mM)
6.76	1.9	0.178	1	0.670	235.1	198.0
6.78	1.86	0.174	1	0.668	235.0	197.8
6.86	0.969	0.092	1	0.673	235.8	200.1
6.83	0.995	0.088	1	0.676	236.0	200.5
6.66	1.8	0.172	7.3	5.111	223.6	199.0
6.65	1.74	0.164	7.3	5.129	223.7	199.4
6.79	0.942	0.092	7.3	5.084	223.9	200.2
6.76	0.951	0.084	7.3	5.114	224.0	200.6
6.57	1.8	0.166	13.7	9.941	210.3	198.4
6.68	1.7	0.157	13.7	9.752	210.2	197.3
6.72	0.898	0.086	13.7	9.855	210.7	199.5
6.7	0.934	0.085	13.7	9.884	210.7	199.7
6.48	1.73	0.160	20	15.002	196.2	197.1
6.48	1.72	0.157	20	15.083	196.0	197.1
6.65	0.89	0.082	20	14.798	196.7	198.0
6.63	0.963	0.085	20	14.828	196.7	197.9

Appendix I: Computing Ionic Species Distribution from Reported Data on Buffer Composition

Comparing model-estimated apparent equilibrium constants to measured values (used here to estimate a consistent set of species-level thermodynamic properties) requires estimating the ionic composition of the buffer associated with each measured equilibrium constant value for each reaction. Here information from original reports is synthesized to generate estimated values of free Na^+, K^+, Ca^{2+}, and Mg^{2+} concentrations, overall ionic strength, pH, and temperature, so that these aspects of the biochemical state are quantified for each raw equilibrium data entry in the database. This appendix briefly describes how these calculations are conducted for two example reactions.

Example 1

Data for glucose-6-phosphate isomerase (EC 5.3.1.9) were obtained from Tewari et al.,[39] which reported equilibrium constants of [ΣF6P]/[ΣG6P] at several different temperatures and ionic conditions. Several different total concentrations of Tris buffer were used to obtain reported pH values of 8.7, as reported in Table A1. The valued listed in the table under "reported conditions" were used to estimate the total concentrations reported under "computed total concentrations", using the following steps:

(1) The concentration of H^+-ion bound Tris ([Tris·H^+]) was computed assuming that Tris does not significantly bind magnesium or sodium ions at the given concentrations:

$$[H^+\cdot\mathrm{Tris}] = [\mathrm{Tris}]\frac{10^{-\mathrm{pH}}/10^{-\mathrm{p}K_{\mathrm{H,Tris}}}}{1 + 10^{-\mathrm{pH}}/10^{-\mathrm{p}K_{\mathrm{H,Tris}}}}$$

The Tris H^+-ion dissociation was assumed to have a pK value of pK_H = 8.072, as reported by Tewari et al.[39]

(2) Added [HCl] used to obtain the reported pH was estimated to be equal to [Tris·H^+]. Thus total chloride ion ($[Cl^-]_{tot}$) was computed from the sum $[Cl^-]_{tot} = [\mathrm{Tris}\cdot H^+] + 2[MgCl_2]$.

(3) Hexose-6P sugars were added as disodium salts in the range 34−55 mM. The calculations here take the average concentration (44.5 mM) to obtain total added sodium ion of 0.089 M. The total hexose-6-phosphate $[H6P]_{tot}$ refers to total [ΣF6P] + [ΣG6P].

Given the total concentrations reported in Table A1, the free unbound concentrations of magnesium ion and

[$H6P^{2-}$] for each entry are calculated from solving the following mass balance equations:

$$[H6P]_{tot} = [H6P^{2-}] + [H\cdot H6P^-] + [Mg\cdot H6P]$$

$$[Mg]_{tot} = [Mg^{2+}] + [Mg\cdot H6P]$$

where the two hexose-6-phosphate sugars are lumped into a single representative reactant, assumed to have the same H^+- and Mg^{2+}-dissociation properties:

$$[H\cdot H6P^-] = [H6P^{2-}]\frac{10^{-\mathrm{pH}}}{10^{-\mathrm{p}K_{\mathrm{H\_H6P}}}}$$

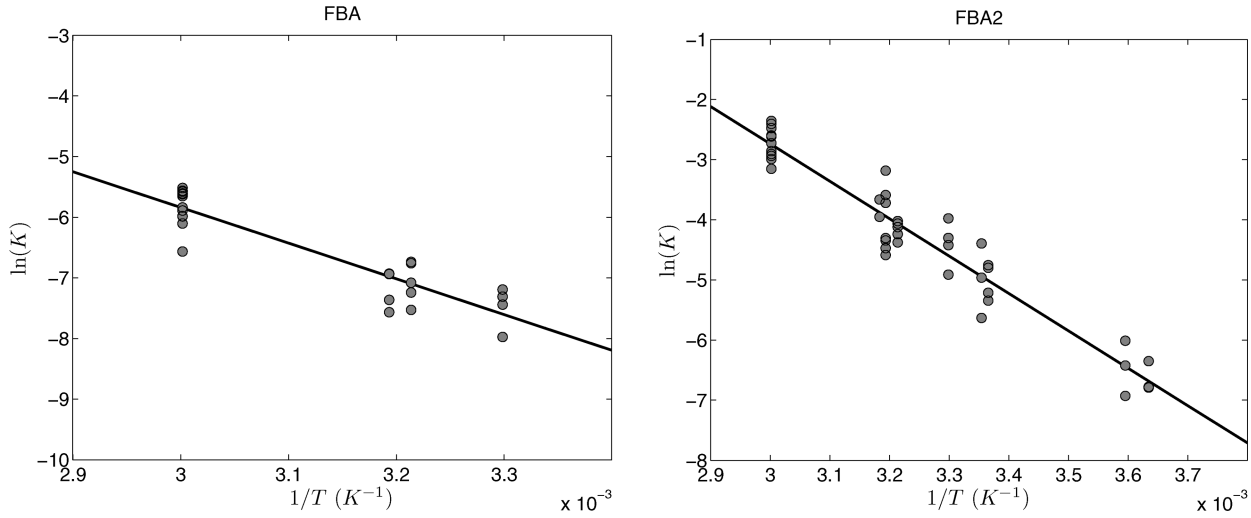

Figure A1. Plot of ln(K) versus 1/T for the fructose-1,6-biphosphatate aldolase (FBA and FBA2) reactions. The data points plotted as solid circles to correspond to $I = 0$. The reaction enthalpies are obtained by multiplying the slope of fitted line by $-R$.

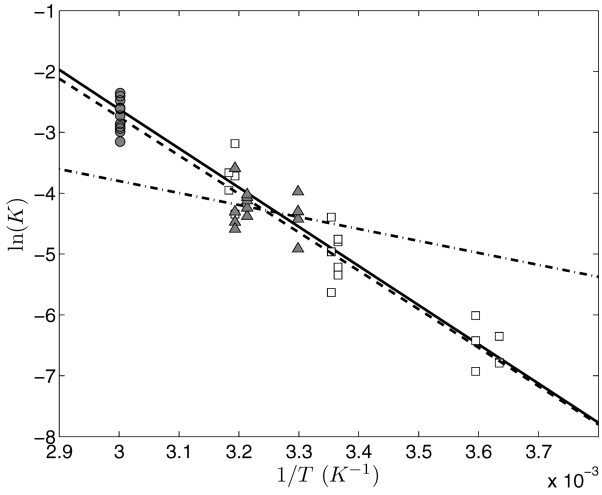

Figure A2. Comparison of Utter et al.[46] and Meyerhof et al.[47] data for the FBA2 reaction. The Utter et al. data are plotted as open squares, and the Meyerhof et al. data are plotted as solid circles for the high-temperature data and as solid triangles for low-temperature data. The linear fit for data set 1 is plotted as a solid line, data set 2 a dashed line, and data set 3 a dot-dash line, where data sets 1, 2, and 3 are defined in Appendix II.

$$[\mathrm{Mg{\cdot}H6P}] = [\mathrm{H6P^{2-}}]\frac{[\mathrm{Mg^{2+}}]}{10^{-\mathrm{p}K_{\mathrm{Mg\_H6P}}}}$$

These mass balance equations assume that Na^+ and Cl^- ions are fully unbound in these experiments. The values of pK_{H_H6P} and pK_{Mg_H6P} are taken as 5.8275 and 1.6150, respectively, corresponding to values in Table 2, adjusted for an ionic strength of 0.153 M, which is close to the value of I estimated for the data entries from Tewari et al.[39] The assumption that G6P and F6P have equivalent H^+- and Mg^{2+}-dissociation properties is consistent with the pK values adopted in this study.

The resulting computed free ion concentrations and ionic strengths are listed in Table A2. The ionic strength of the solution is calculated by the following equation:

$$I = \frac{1}{2}(4[\mathrm{H6P^{2-}}] + [\mathrm{H{\cdot}H6P^-}] + [\mathrm{Cl^-}] + [\mathrm{Tris{\cdot}H^+}] + 4[\mathrm{Mg^{2+}}] + [\mathrm{Na^+}] + [\mathrm{H^+}])$$

Example 2

Data for phosphoglycerate mutase (EC 5.4.2.1) are obtained from Guynn,[40] in which equilibrium was approached from both sides of the reaction at various concentrations of magnesium and added KCl to reach a target ionic strength of 0.25 in a 25 mM phosphate buffer at a temperature of 311.15 K. Total final PG2, PG3, added magnesium in the form of $MgCl_2$, and measured final pH were reported (Table A3). The phosphoglycerates and inorganic phosphate in the solution exist in unbound anionic forms, proton, magnesium, and potassium ion bound forms.

In this example, the solution composition may be computed by applying both mass and charge conservation equations, as follows. For each biochemical measurement entry, the total added magnesium is fixed at a constant given by the reported added $MgCl_2$.

$$\mathrm{Mg_{tot}} = [\mathrm{Mg^{2+}}] + [\mathrm{Mg{\cdot}PG2^-}] + [\mathrm{Mg{\cdot}PG3^-}] + [\mathrm{Mg{\cdot}HPO_4}] + [\mathrm{Mg{\cdot}H_2PO_4^+}]$$

The ionic strength of the solution was adjusted to the specified value of $I_{\mathrm{target}} = 0.25$ M:

$$\begin{aligned} I_{\mathrm{target}} = \frac{1}{2}([\mathrm{K^+}] + [\mathrm{Cl^-}] + 4[\mathrm{Mg^{2+}}] + 4[\mathrm{HPO_4^{2-}}] + [\mathrm{H_2PO_4^-}] + \\ [\mathrm{Mg{\cdot}H_2PO_4^+}] + [\mathrm{K{\cdot}HPO_4^-}] + 9[\mathrm{PG2^{3-}}] + 4[\mathrm{H{\cdot}PG2^{2-}}] + \\ [\mathrm{Mg{\cdot}PG2^-}] + 4[\mathrm{K{\cdot}PG2^{2-}}] + 9[\mathrm{PG3^{3-}}] + 4[\mathrm{H{\cdot}PG3^{2-}}] + \\ [\mathrm{Mg{\cdot}PG3^-}] + 4[\mathrm{K{\cdot}PG3^{2-}}] + [\mathrm{H^+}] + [\mathrm{OH^-}]) \end{aligned}$$

The total charge in the system must be conserved:

$$\begin{aligned} 0 = [\mathrm{K^+}] - [\mathrm{Cl^-}] + 2[\mathrm{Mg^{2+}}] - 2[\mathrm{HPO_4^{2-}}] - [\mathrm{H_2PO_4^-}] + \\ [\mathrm{Mg{\cdot}H_2PO_4^+}] - [\mathrm{K{\cdot}HPO_4^-}] - 3[\mathrm{PG2^{3-}}] - 2[\mathrm{H{\cdot}PG2^{2-}}] - \\ [\mathrm{Mg{\cdot}PG2^-}] - 2[\mathrm{K{\cdot}PG2^{2-}}] - 3[\mathrm{PG3^{3-}}] - 2[\mathrm{H{\cdot}PG3^{2-}}] - \\ [\mathrm{Mg{\cdot}PG3^-}] - 2[\mathrm{K{\cdot}PG3^{2-}}] + [\mathrm{H^+}] - [\mathrm{OH^-}] \end{aligned}$$

The unknowns determined in this system are $[Mg^{2+}]$, $[K^+]$, and $[Cl^-]$. The ionic species concentrations in these three conservation equations are computed as functions of the free ion concentrations and the total biochemical reactant concentrations

based on the dissociation constants reported in Table 2, adjusted to $T = 311.15$ K and $I = 0.25$ M.

Note that both total and free $[K^+]$ exceed $[Cl^-]$ because the phosphoglycerates were added as potassium salts and the 25 mM phosphate buffer is based on potassium salts of phosphate (Table A3).

Appendix II: Estimating the Standard Reaction Enthalpy ($\Delta_r H°$) from Experimentally Measured Apparent Equilibrium Constants (K')

Measurements of apparent equilibrium constants at different temperatures are available in the raw-data database for 10 of the 25 reactions studied here (as shown in Table 1 in the paper). For these cases apparent equilibrium constants measured at multiple temperatures allow for direct estimates of the reaction enthalpy. To obtain $\Delta_r H°$, we first compute ionic species distribution and ionic strength of buffer under experimental conditions as described in Appendix I and then compute the equilibrium constants of corresponding reference reactions at zero ionic strength based on the procedure listed in the methods. By assuming that $\Delta_r H°$ is independent of temperature over experimental temperature ranges, we can obtain $\Delta_r H°$ from the linear relationship between $\ln(K)$ and $1/T$ (i.e., van't Hoff relationship):

$$\frac{\mathrm{d}\ln(K)}{\mathrm{d}(1/T)} = -\frac{\Delta_r H°}{R} \qquad \text{(A1)}$$

Examples of computing $\Delta_r H°$ of the reactions of fructose-1,6-biophosphatate aldolase (FBA), fructose-1,6-biophosphatate aldolase 2 (FBA2), and triosphosphate isomerase (TPI) are illustrated below.

Example 1

The biochemical reactions of FBA, FBA2, and TPI are shown in Table 1. Literature-reported K' of reactions of FBA and FBA2 are available in the Goldberg et al. database,[27] which includes the K' of FBA2 measured by Utter et al.[46] at multiple temperatures ranging from 275.15 to 314.15 K, and the K' of FBA and FBA2 determined by Meyerhof et al.[47] at temperatures ranging from 303.15 to 333.15 K. Ion concentrations are estimated on the basis of specified experimental conditions, and reference-reaction equilibrium constants at zero ionic strength K estimated for the Utter et al. and Meyerhof et al. measurements.

Linear regressions of $\ln(K)$ versus $1/T$ are plotted in Figure A1 as solid lines along with data for FBA and FBA2. The $\Delta_r H°$ for FBA and FBA2 are computed from the slopes according to eq A1. Because the TPI reaction is stoichiometrically equivalent to the combination of FBA and FBA2, the associated $\Delta_r H°$ is computed as

$$\Delta_r H°(\mathrm{TPI}) = \Delta_r H°(\mathrm{FBA2}) - \Delta_r H°(\mathrm{FBA}) = 2.73\ (\mathrm{kJ/mol})$$

These values of $\Delta_r H°$ are based on data from Meyerhof et al. that were obtained at temperatures as high as 333.15 K, which exceeds the defined valid temperature range (273.15 to 313.15 K) of the extended Debye−Hückel theory.[11,31,33] To investigate the validity of including of the 333.15K data in the computation, let us perform linear regressions for FBA2 reaction for different sets of data sets, including the Utter et al. data (data set 1), the Meyerhof et al. data including the high-temperature data (data set 2), and the Meyerhof et al. data excluding the high-temperature data (data set 3). The linear regressions for the three data sets are plotted as solid, dashed, and dot-dash lines, respectively, in Figure A2, and the corresponding computed $\Delta_r H°$ are 53.59, 52.52, and 16.34 kJ/mol. Because the difference in estimated $\Delta_r H°$ between data set 1 and data set 2 is much smaller than that between data set 1 and data set 3, and because data set 1 is obtained with the well-defined temperature range, we conclude that the inclusion of Meyerhof et al. high-temperature data improves the accuracy of the estimation of $\Delta_r H°$. Thus we choose to include the Meyerhof et al. high-temperature (333.15K) data in estimating $\Delta_r H°$ for FBA and FBA2.

Nomenclature

a	activity
B	an empirical constant taken to be 1.6 $M^{-1/2}$
$\Delta_r G°$	standard Gibbs free energy of reaction
$\Delta_f G_i°$	standard Gibbs free energy of formation of species i
$\Delta_d H_{K_d}$	enthalpy of proton/metal cation dissociation
$\Delta_r H°$	standard enthalpy of reaction
I	ionic strength
K_d	dissociation constant
K'	apparent equilibrium constant
K	chemical (reference reaction) equilibrium constant
N	the total number of species
P_j	binding polynomial associated with reactant j
pK	negative logarithm of the dissociation constant
R	gas constant, 8.3145 $J \cdot K^{-1} \cdot mol^{-1}$
γ	activity coefficient
T	temperature
υ_i	stoichiometric coefficient for species i in a given reaction
z_i	charge number of species i

References and Notes

(1) Vojinović, V.; von Stockar, U. *Biotechnol. Bioeng.* **2009**, *103*, 780.
(2) Goldberg, R. N.; Tewari, Y. B.; Bell, D.; Fazio, K.; Anderson, E. *J. Phys. Chem. Ref. Data* **1993**, *22*, 515.
(3) Schuster, R.; Schuster, S. *Comput. Appl. Biosci.* **1993**, *9*, 79.
(4) Bonarius, H. P. J.; Schmid, G.; Tramper, J. *Trends Biotechnol.* **1997**, *15*, 308.
(5) Mavrovouniotis, M. L. Identification of localized and distributed bottlenecks in metabolic pathways. In *Proceedings of the 1st Int. Conf. on Intelligent Systems for Molecular Biology*; AAAI: Bethesda, MA, 1993; pp 275.
(6) Yang, F.; Beard, D. A. *Biophys. Chem.* **2006**, *120*, 121.
(7) Kümmel, A.; Panke, S.; Heinemann, M. *Mol. Syst. Biol.* **2006**, *2*, 2006–0034.
(8) Henry, C. S.; Broadbelt, L. J.; Hatzimanikatis, V. *Biophys. J.* **2007**, *92*, 1792.
(9) Vinnakota, K. C.; Wu, F.; Kushmerick, M. J.; Beard, D. A. *Methods Enzymol.* **2009**, *454*, 29.
(10) Vinnakota, K.; Kemp, M. L.; Kushmerick, M. J. *Biophys. J.* **2006**, *91*, 1264.
(11) Alberty, R. A. *Thermodynamics of Biochemical Reactions*; Wiley-Interscience: Hoboken, NJ, 2003.
(12) Alberty, R. A. *Proc. Natl. Acad. Sci U.S.A.* **1991**, *88*, 3268.
(13) Alberty, R. A. *Biophys. Chem.* **1992**, *42*, 117.
(14) Alberty, R. A. *Biochim. Biophys. Acta* **1994**, *1207*, 1.
(15) Alberty, R. A. *Biophys. Chem.* **2005**, *114*, 115.
(16) Alberty, R. A. *Biophys. Chem.* **2006**, *122*, 74.
(17) Alberty, R. A. *Biochemistry* **2006**, *45*, 15838.
(18) Alberty, R. A. *Arch. Biochem. Biophys.* **2006**, *451*, 17.
(19) Alberty, R. A. *Biophys. Chem.* **2007**, *127*, 91.
(20) Goldberg, R. N.; Tewari, Y. B.; Bhat, T. N. *Bioinformatics* **2004**, *20*, 2874.
(21) Wu, F.; Yang, F.; Vinnakota, K. C.; Beard, D. A. *J. Biol. Chem.* **2007**, *282*, 24525.
(22) Qi, F.; Chen, X.; Beard, D. A. *Biochim. Biophys. Acta* **2008**, *1784*, 1641.
(23) Wu, F.; Zhang, J.; Beard, D. A. *Proc. Natl. Acad. Sci.* **2009**, *106*, 7143.

(24) Goldberg, R. N.; Tewari, Y. B. *J. Phys. Chem. Ref. Data* **1989**, *18*, 809.
(25) Goldberg, R. N.; Tewari, Y. B. *J. Phys. Chem. Ref. Data* **1994**, *23*, 547.
(26) Goldberg, R. N.; Tewari, Y. B. *J. Phys. Chem. Ref. Data* **1994**, *23*, 1035.
(27) Goldberg, R. N.; Tewari, Y. B. *J. Phys. Chem. Ref. Data* **1995**, *24*, 1669.
(28) Goldberg, R. N.; Tewari, Y. B. *J. Phys. Chem. Ref. Data* **1995**, *24*, 1765.
(29) Goldberg, R. N. *J. Phys. Chem. Ref. Data* **1999**, *28*, 931.
(30) Goldberg, R. N.; Tewari, Y. B.; Bhat, T. N. *J. Phys. Chem. Ref. Data* **2007**, *36*, 1347.
(31) Beard, D. A.; Qian, H. Conventions and calculations for biochemical systems. In *Chemical Biophysics: Quantitative Analysis of Cellular Systems*; Cambridge University Press: Cambridge, U.K., 2008; pp 24.
(32) Alberty, R. A. *J. Phys. Chem. B* **2006**, *110*, 5012.
(33) Clarke, E. C. W.; Glew, D. N. *J. Chem. Soc., Faraday Trans. 1* **1980**, *76*, 1911.
(34) Alberty, R. A. *J. Phys. Chem. B* **2001**, *105*, 7865.
(35) Alberty, R. A. *J. Phys. Chem. B* **2001**, *105*, 1109.
(36) Alberty, R. A. *J. Phys. Chem. B* **2005**, *109*, 9132.
(37) Rosing, J.; Slater, E. C. *Biochim. Biophys. Acta* **1972**, *267*, 275.
(38) Dobson, G. P.; Hitchins, S.; Teague, W. E., Jr. *J. Biol. Chem.* **2002**, *277*, 27176.
(39) Tewari, Y. B.; Steckler, D. K.; Goldberg, R. N. *J. Biol. Chem.* **1988**, *263*, 3664.
(40) Guynn, R. W. *Arch. Biochem. Biophys.* **1982**, *218*, 14.
(41) Vanlier, J.; Wu, F.; Qi, F.; Vinnakota, K. C.; Han, Y.; Dash, R. K.; Yang, F.; Beard, D. A. *Bioinformatics* **2009**, *25*, 836.
(42) Guyton, A. C.; Hall, J. E. Transport of substances through the cell membrane. In *Textbook of Medical Physiology*; W. B. Saunders: Philadelphia, PA, 2000; p 40.
(43) Godt, R. E.; Maughan, D. W. *Am. J. Physiol. Cell Physiol.* **1988**, *254*, C591.
(44) Kammermeier, H.; Schmidt, P.; Jüngling, E. *J. Mol. Cell. Cardiol.* **1982**, *14*, 267.
(45) Phillips, R. C.; George, S. J. P.; Rutman, R. J. *J. Am. Chem. Soc.* **1966**, *88*, 2631.
(46) Utter, M. F.; Werkman, C. H. *J. Bacteriol.* **1941**, *42*, 665.
(47) Meyerhof, O.; Junowicz-Kocholaty, R. *J. Biol. Chem.* **1943**, *149*, 71.
(48) Martell, A. E.; Smith, R. M.; Motekaitis, R. J. *NIST Standard Reference Database 46 Version 8.0: NIST Critically Selected Stability Constants of Metal Complexes*; NIST Standard Reference Data: Gaithersburg, MD, 2004.
(49) Alberty, R. A. *J. Phys. Chem.* **1995**, *99*, 11028.
(50) Tewari, Y. B.; Steckler, D. K.; Goldberg, R. N.; Gitomer, W. L. *J. Biol. Chem.* **1988**, *263*, 3670.
(51) Larsson-Raünikiewicz, M. *Eur. J. Biochem.* **1972**, *30*, 579.
(52) Merrill, D. K.; McAlexander, J. C.; Guynn, R. W. *Arch. Biochem. Biophys.* **1981**, *212*, 717.

JP911381P